Characterization and Thermomechanical Processing of Sprayformed Allvac® 720 Alloy

Henry E. Lippard and Robin Forbes Jones
Allvac
An Allegheny Technologies Company

Sprayforming is a promising route for production of highly segregation prone alloys such as the high γ′ fraction nickel alloys that are finding increased usage in the hot stages of aircraft turbines. Conventional ingot metallurgy (IM) is experiencing increasing difficulties with segregation and segregation-related defects such as freckles and white spots with the highly alloyed materials and probably will not be able to produce the next generation of hot stage alloys. Powder metallurgy (PM) is an expensive production route and the oxide cleanliness is inferior to IM. Sprayforming offers the segregation free microstructure of PM with the oxide cleanliness of IM through the clean metal sprayforming (CMSF) technique at a production cost intermediate between IM and PM.

Sprayformed Allvac® 720 Alloy was produced by nitrogen gas atomization and collected as 325 mm diameter billets. The nitrogen atomization eliminated the thermal induced porosity typical of powder metallurgy production using argon atomization and refined the initial structure relative to conventional cast material. The as-sprayed grain size is an equiaxed ASTM 6-7 and the carbonitride particle distribution is 1-2 μm. No segregation or segregation-related defects such as freckles or white spots were observed.

The response of sprayformed material to thermomechanical processing (TMP) is demonstrated by an experimental forging matrix measuring the effects of heat treatment, strain, and strain rate. The sprayformed material exhibits a strong recrystallization response and the only unrecrystallized grains are observed in low strain rate deformation conditions. The deformation temperature and strain rate are the primary variables affecting the flow stress and the prior heat treatment has a minor effect at lower temperatures in the hot working range.

Superalloys 2000
Edited by T.M. Pollock, R.D. Kissinger, R.R. Bowman,
K.A. Green, M. McLean, S. Olson, and J.J. Schirra
TMS (The Minerals, Metals & Materials Society), 2000

Introduction

The sprayforming production method is a competing manufacturing process to powder metallurgy (PM) and conventional ingot metallurgy (IM) for nickel-base superalloys. The sprayforming process in the simplest terms is atomization of a molten metal stream and collection of the resulting droplets in a "preform", which is analogous to an ingot. The atomization process is similar to powder metallurgy techniques but the droplets are not allowed to completely solidify before collection as a preform. The droplets are typically collected in a 60%-80% solid fraction range on a rotating starter plate that is withdrawn as the preform lengthens to maintain a constant deposition plane distance from the nozzle. The system complexity is quite high and the major variables are atomizing gas, atomizer design, gas:metal ratio, preform rotation speed, nozzle raster pattern, nozzle to preform distance, and molten metal pour rate.

Experimental Procedure

The preforms were sprayed in the United Kingdom by Osprey Metals Ltd* on pilot plant scale equipment with a 1200 kg melting capacity. The preforms were atomized with nitrogen gas to ensure any residual porosity or gas pockets would fully dissolve in the alloy and not reappear as thermal induced porosity at high temperatures. The nozzle experienced some clogging during the spray run that lowered the metal pour rate; thus the gas flow rate was reduced to maintain a constant gas:metal ratio. The as-sprayed preform sizes were 325 mm Ø x 1385 mm and 325 mm Ø x 880 mm length.

The preforms were sampled in steady-state regions near each end to provide the specimens for this study. The bulk of the preforms will be forged to billet based on these subscale processing results. The Gleeble compression specimens were heat treated to produce γ' dispersions A or B, then machined to 10 mm Ø x 15 mm length cylinders. The specimens were heated in an argon atmosphere at 10°C/s to the test temperature and then held for 5 minutes to equilibrate. The deformation was conducted in four steps of 0.2 true strain each with a one minute dwell time after each strain step. The specimens were water quenched after the final one minute hold to preserve the dynamic microstructure. The samples were sectioned, polished, and etched to reveal the centerline longitudinal plane for optical and SEM analysis.

Results and Discussion

The chemistry analyses listed in Table I demonstrate that no macrosegregation occurred during the sprayforming process. A microchemical analysis by energy dispersive spectrometry (EDS) compared the composition of the grain centers and boundaries to detect microsegregation, Table II. The composition differences between the grain centers and boundaries were not statistically significant above a 1σ range for the EDS measurement error nor did they exceed a customary definition of 5% difference for microsegregation. None of the major alloying elements are highly segregation prone and thus, Allvac® 720 Alloy is an ideal sprayforming candidate.

The high nitrogen level is consistent with absorption of the atomizing gas in the atomizing zone and as a hot preform. The center region remains higher in temperature due to the insulating effects of the outer preform layers and thus has higher nitrogen solubility. The top of the preform is also better insulated by the bottom of the preform relative to the initial starting conditions of the cold starter plate. The higher oxygen content in the preform bottom region is due to the initial air atmosphere in the spray chamber that becomes increasingly nitrogen rich as the spray time increases.

Table I Chemistry as a function of Preform Location

	Top		Bottom	
(wt%)	Surface	Center	Surface	Center
Ni	57.37	57.38	57.37	57.36
Cr	15.92	15.93	15.92	15.93
Co	14.50	14.49	14.52	14.54
Ti	5.00	4.98	5.00	4.99
Mo	3.03	3.03	3.03	3.03
Al	2.60	2.60	2.61	2.59
W	1.23	1.23	1.22	1.23
Fe	0.18	0.18	0.15	0.15
V	0.06	0.06	0.06	0.06
Zr	0.04	0.04	0.04	0.04
Ta	0.02	0.03	0.03	0.03
Nb	0.01	0.01	0.01	0.01
Si	0.01	0.01	0.01	0.01
Mn	0.01	0.01	0.01	0.01
Cu	0.01	0.01	0.01	0.01
B	0.015	0.014	0.015	0.015
C	0.016	0.016	0.014	0.016
N	0.0305	0.0320	0.0185	0.0257
O	0.0028	0.0026	0.0050	0.0047
P	0.003	0.004	0.003	0.003
S	<.0003	<.0003	<.0003	<.0003

Table II EDS Measurement of Microsegregation

	Avg. Grain Composition (wt%)			EDS +/-
	Center	Boundary	GC-GB	1σ range
Ni	57.05	57.68	-0.63	1.58
Cr	16.64	16.18	0.45	0.47
Co	15.00	14.62	0.38	0.96
Ti	4.74	4.95	-0.21	0.29
Mo	2.86	2.75	0.11	0.33
Al	2.23	2.31	-0.08	0.23
W	1.50	1.53	-0.03	0.34

The microstructure of the as-sprayed preform was similarly characterized as a function of location. Table III quantifies the grain size and carbonitride dispersions. Figure 1 shows the equiaxed grain structure inherent to the sprayforming process and illustrates the effects of the higher core temperature through the coarser grain size and decreased porosity at the preform center. The carbonitride dispersion is also coarser in the center and the particle aspect ratio is reduced.

Table III As-sprayed Microstructure of Alloy 720 Preform

	Surface	Center
Top		
Grain Size (ASTM)	7	6
Bottom		
Grain Size (ASTM)	7	6
Carbide Size (μm)		
Width, std. dev.	0.6 , 0.2	1.0 , 0.4
Length, std. dev.	1.1 , 0.4	1.3 , 0.5
Aspect Ratio, std. dev.	1.9 , 0.7	1.3 , 0.3

* Osprey Metals Ltd
Red Jacket Works
United Kingdom

The γ′ dispersions, A and B, are shown in Figures 2 and 3, respectively. The A γ′ dispersion consists of fine, intragranular rounded cuboids ranging from 0.8 μm – 1.2 μm diameter and the grain boundaries are partially outlined with particles that range up to 10 μm in length and 3 μm width. The B dispersion has a coarser, intragranular butterfly type particle and the grain boundaries are outlined with coarser particles that reach 20 μm length x 6 μm width. The butterfly particles are ~4 μm in width and their shape is indicative of solid state dendritic arm growth. The coarser grain boundary γ′ also increased the width of the precipitate free zone adjacent to the grain boundaries. Both dispersions were created by subsolvus slow cooling cycles with the same initial (2000°F) and final (1900°F) temperatures; however, the B specimens were cooled at a slower rate to produce the coarser microstructure.

The recrystallization response measured by grain size is listed in Table IV. The experimental variables covered the full range of practical thermomechanical processing parameters. The deformation temperature spans from near γ′ (sub)solvus to the temperature required to produce fine grain forging billet material. The strain rate spans from the typical draw forging rates to the slowest upset forging rates. The heat treatment is designed to coarsen the γ′ dispersion, which enhances the hot workability and recrystallization response.

The forging temperature was the only variable that significantly affected the recrystallization response. The preforging heat treatment and deformation strain rate did not consistently influence the recrystallized grain size. The decreasing deformation temperature increased the precipitated γ′ volume fraction that pinned the recrystallized grains at smaller sizes. Figure 4 captures the microstructural evolution in a transient condition after forging the B γ′ dispersion at strain rate 1.0 and 1066°C. The distinguishable grain size is ASTM 11 but many regions are in a non-equilibrium recrystallization and grain growth phase. These regions have many small, recrystallized grains less than 1 μm in diameter that consume one another until reaching an equilibrium grain size determined by the forging (holding) temperature. Figure 5 illustrates the microstructure evolution at higher temperatures (1121°C, strain rate 1.0, γ′ dispersion A) where the kinetics are more rapid and the precipitated γ′ volume fraction lower, which produces a larger equilibrium grain size. The striking feature is linear, submicron γ′ precipitate structures extending across all or most of the grain boundary width. These structures may originate from the combination of metastable stacking faults and favorable γ′ precipitation kinetics that preserve the stacking faults. No other specimens in the study exhibited this phenomenon.

All experimental conditions produced fully recrystallized structures except the A γ′ dispersion specimens compressed at 0.03 strain rate in the 1066°C – 1093°C temperature range. Those three conditions had elongated, unrecrystallized grains present but at less than 0.05 area fraction. The coarser B γ′ dispersion appears to enhance the fraction of recrystallization for a given amount of strain but the effect is relatively modest.

A secondary priority after the recrystallization response is minimization of the flow stress to lower the press tonnage required for forging. The peak flow stresses, summarized in Table V, show the strong influence of strain rate and a secondary effect from the γ′ dispersion. Decreasing the strain rate from 1.0 to 0.03 produced an average 97 MPa decrease in the peak flow stress. The γ′ dispersion effect is small (<10%) at near solvus temperatures and at the slower 0.03 strain rate. However, in the 1.0 strain rate and the 1066°C – 1079°C processing range, the B γ′ dispersion flow stress is significantly higher than the A γ′ dispersion. The complete flow stress relationship with true strain is shown in Figure 6 with examples to illustrate the effect of γ′ dispersion, temperature, and strain rate. A feature common to each specimen is the discontinuity in the flow stress after the first 0.2 strain step. The second deformation step always starts at 40-50 MPa lower flow stress than the first step had been completed. This indicates some metadynamic recrystallization occurs during the one minute hold after the first deformation step. The initial flow stresses of the third and fourth deformation steps normally follow the trend established by the previous step or show a maximum discontinuity of 20 MPa.

Table IV Recrystallization of Gleeble specimens forged to 4x0.2 true strain with a one minute hold after each compression step

Temp.	Strain Rate	Heat Treatment	Grain Size	Avg. Grain Size @ Temp.
1066°C	0.03	A	12 ala 9	11
	0.03	B	10.5	
	1.0	A	10	
	1.0	B	11	
1079°C	0.03	A	11 ala 9	10.5
	0.03	B	9.5	
	1.0	A	10.5	
	1.0	B	10.5	
1093°C	0.03	A	10 ala 8	10
	0.03	B	9.5	
	1.0	A	10	
	1.0	B	9.5	
1107°C	0.03	A	8	8.5
	0.03	B	8	
	1.0	A	8.5	
	1.0	B	9	
1121°C	0.03	A	6.5	7
	0.03	B	5.5	
	1.0	A	7.5	
	1.0	B	8	

Table V Peak Flow Stress (MPa) from compression specimens

γ′ Dispersion	A		B	
Strain Rate	0.03	1.0	0.03	1.0
1066°C	236	296	245	344
1079°C	194	297	212	321
1093°C	192	293	195	290
1107°C	172	282	159	270
1121°C	143	240	148	230

Conclusions

Sprayform production of Allvac® 720 Alloy yielded a high quality preform free from macro- and microsegregation. The as-sprayed structure is intermediate between conventional ingot metallurgy and powder metallurgy with an equiaxed ASTM 6-7 grain size and carbonitrides ~1 μm in diameter. These results demonstrate Allvac® 720 Alloy is an ideal candidate alloy for sprayform processing.

The fully recrystallized structures obtained in response to 0.8 true strain in the typical hot working temperature range indicate the thermomechanical processing advantages sprayformed material will possess relative to conventional ingot metallurgy material due to the finer initial structure.

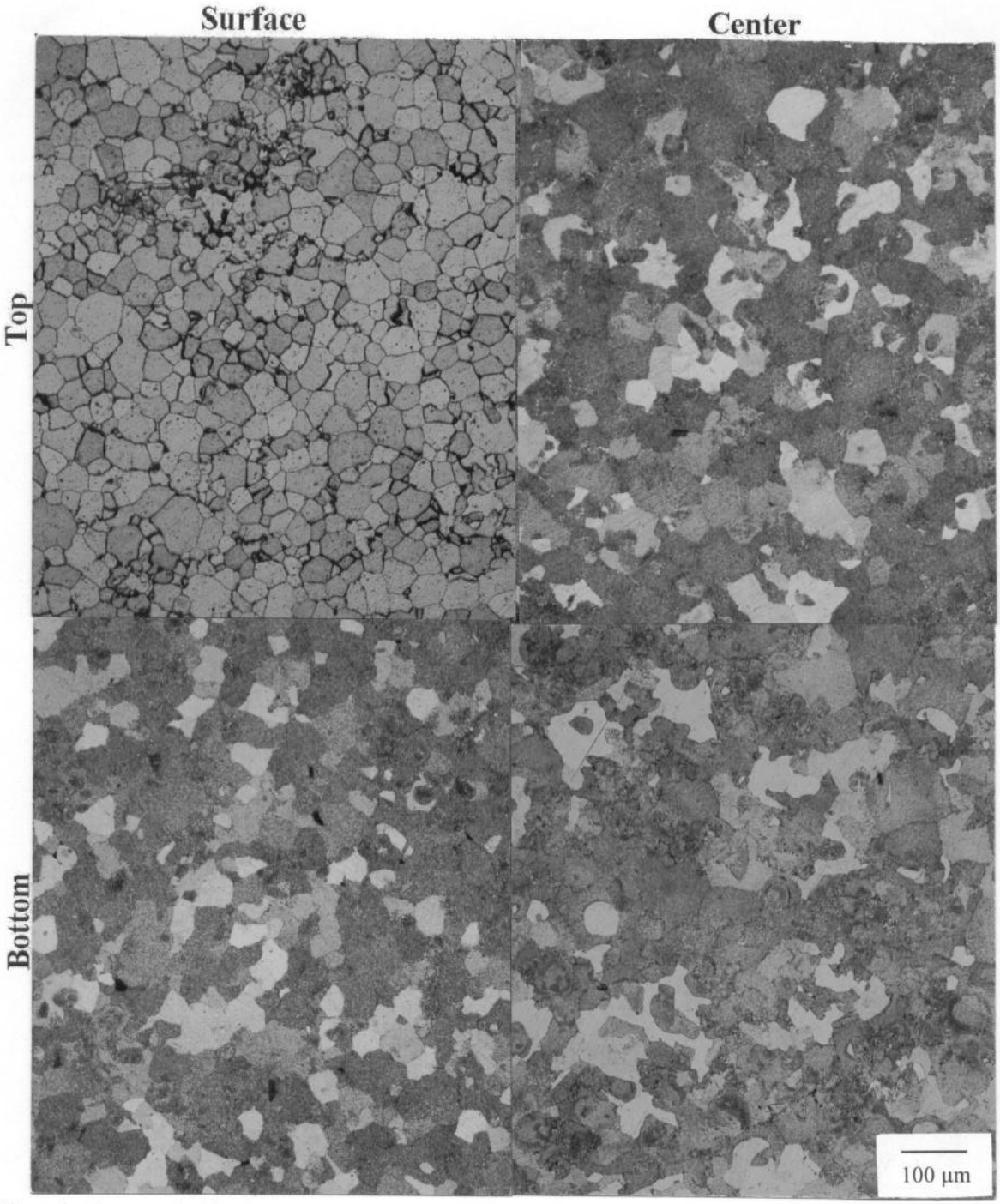

Figure 1: As-sprayed grain structure as a function of location.

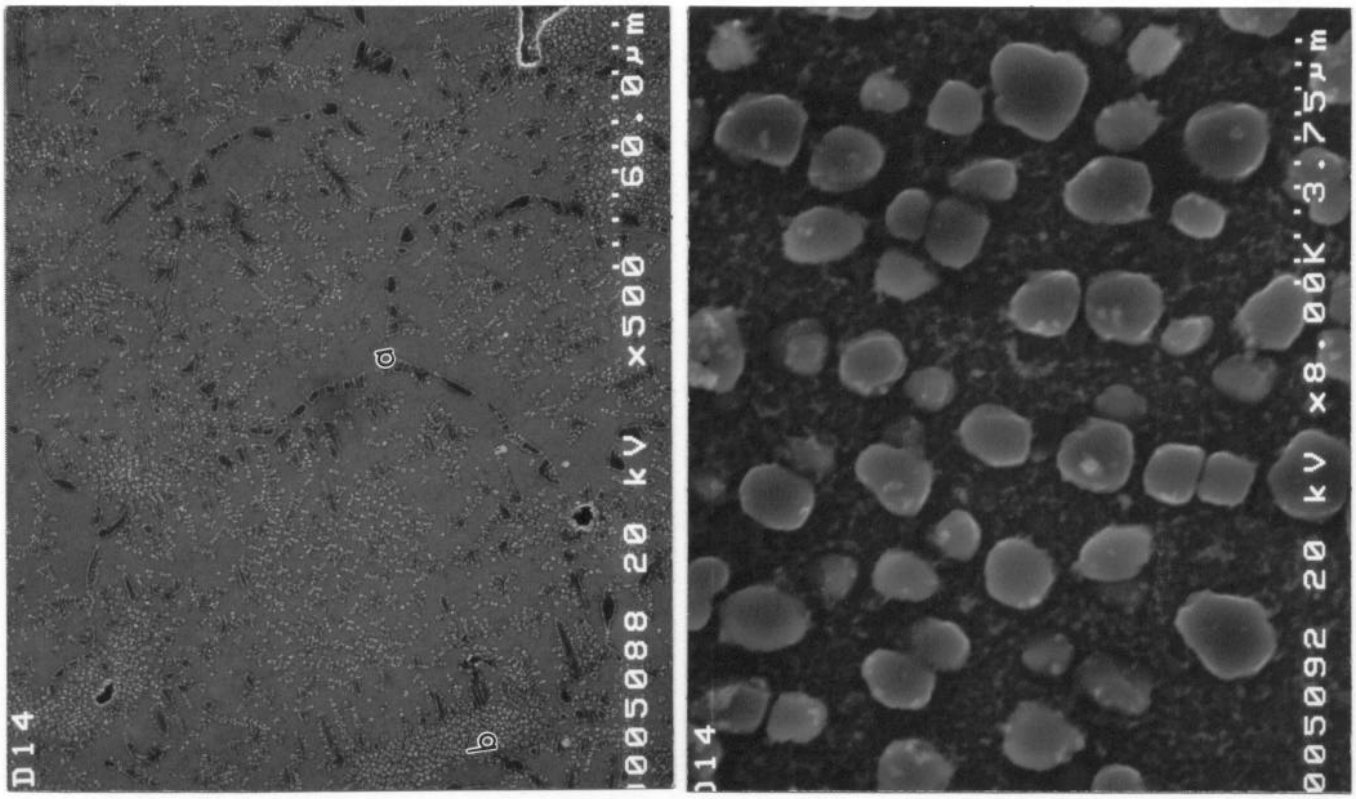

Figure 2: γ′ dispersion produced by heat treatment A.

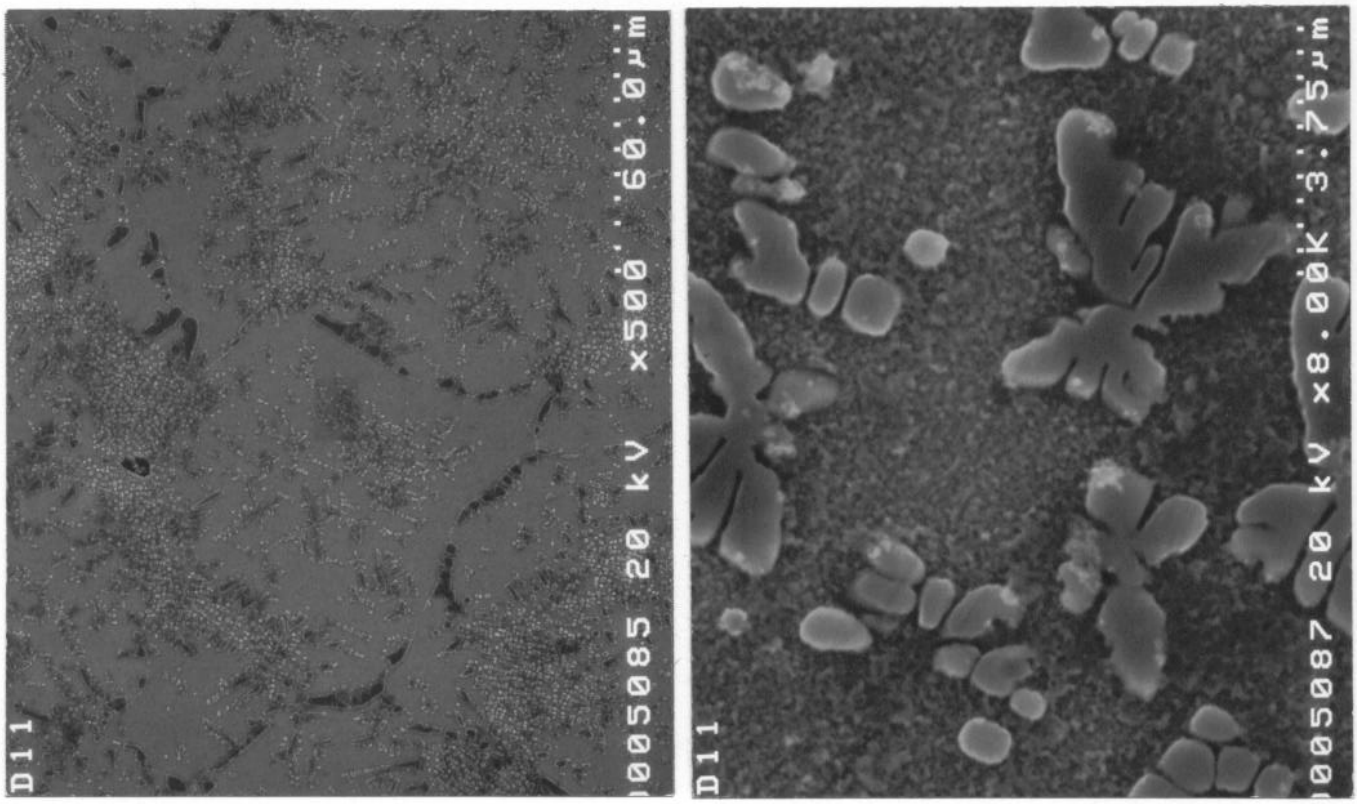

Figure 3: γ′ dispersion produced by heat treatment B.

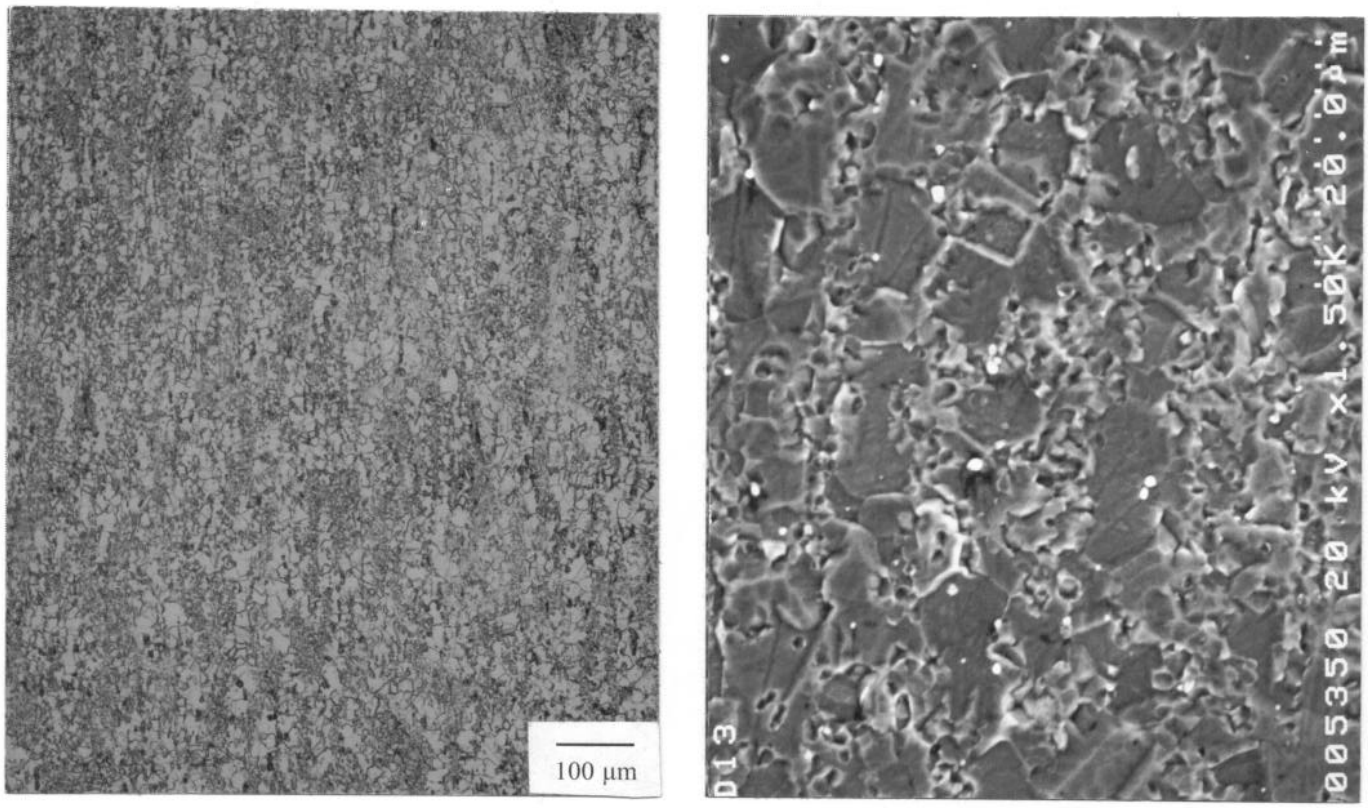

Figure 4: Recrystallization response of Gleeble specimen forged at 1066°C / strain rate 1.0 / γ′ dispersion B.

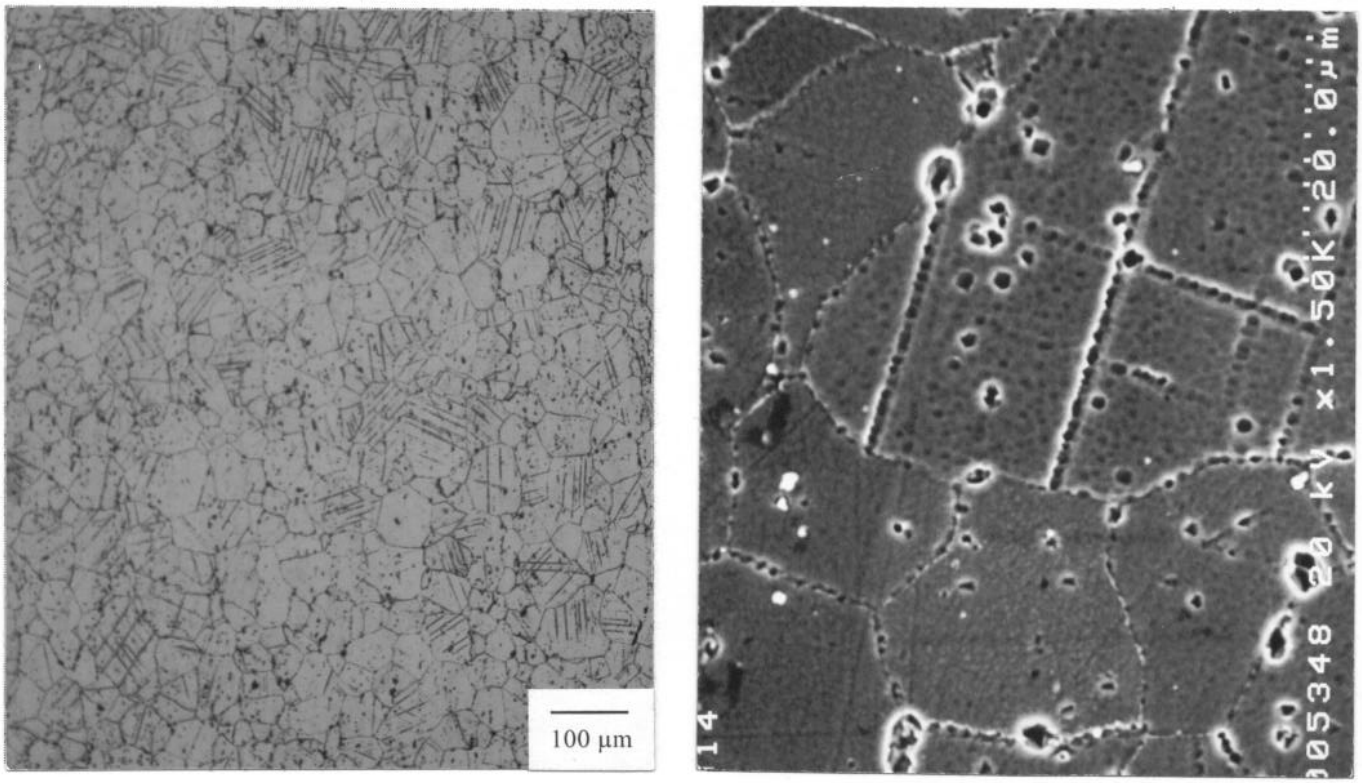

Figure 5: Recrystallization response of Gleeble specimen forged at 1121°C / strain rate 1.0 / γ′ dispersion A.

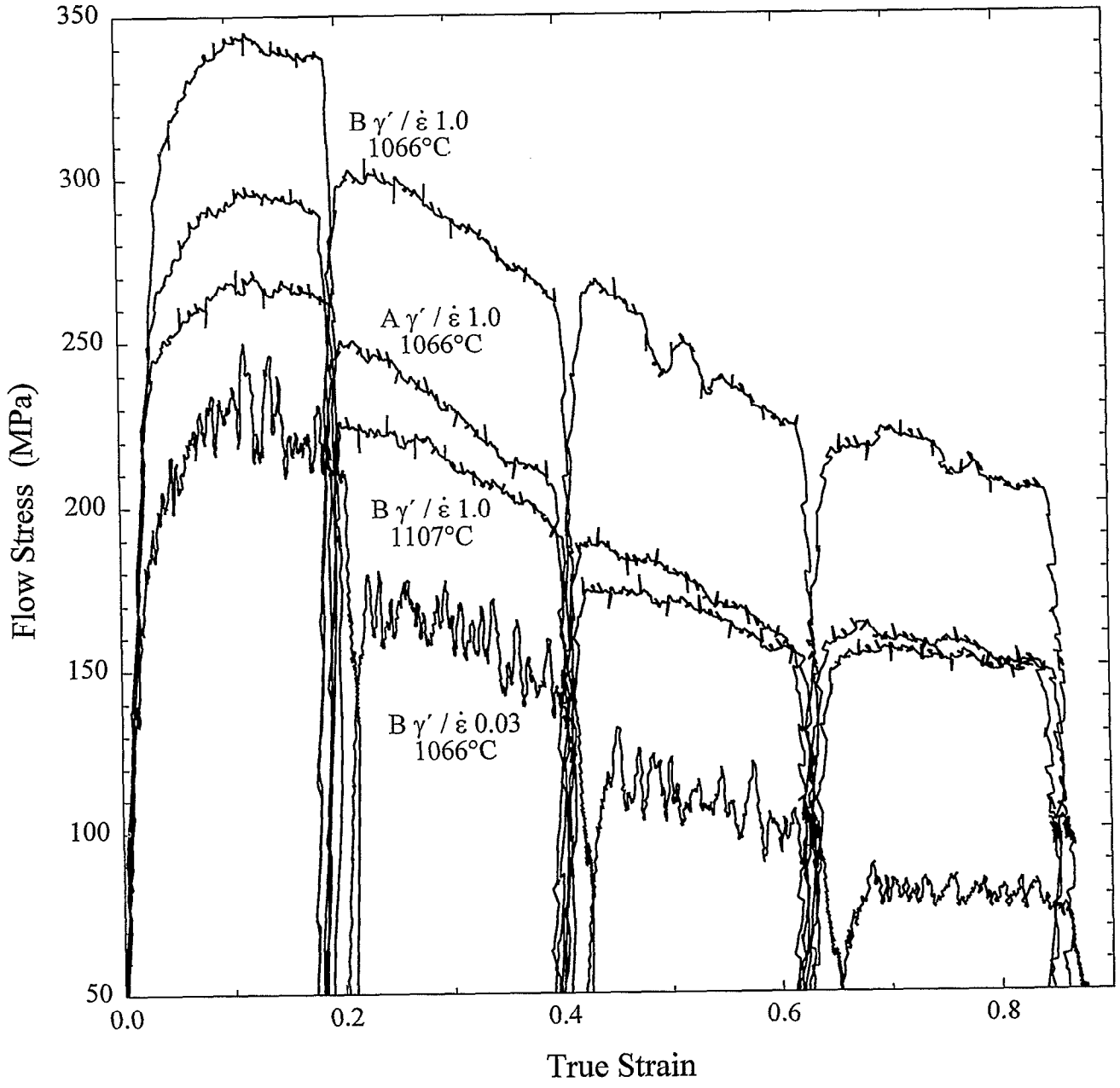

Figure 6: Flow stress as function of true strain from Gleeble compression tests.

Acknowledgements

This work is part of a US Air Force development program with Allvac and General Electric as industry partners. The work is partially funded by US Air Force Dual Use Science and Technology (DUS&T) Agreement Number F33615-99-2-5208 and administered by Mr. Rollie Dutton from Wright-Patterson Air Force Base.